Defect and Diffusion Forum *Online: 2009-03-02*
ISSN: 1662-9507, Vols. 283-286, pp 406-412
doi:10.4028/www.scientific.net/DDF.283-286.406

Synthesis and Characterization of Single Crystals $Y_3Fe_5O_{12}$ and $Bi_3Fe_5O_{12}$ Prepared via Sol Gel Technique

Noorhana Binti Yahya [1, a], Krzysztof K.K. Koziol [2,b] and Mohd Kamarulzaman Bin Mansor[3,c]

[1]Electrical and Electronic Engineering Department, Universiti Teknologi Petronas
Bandar Seri Iskandar, 31750 Tronoh, Perak, Malaysia
[2]Department of Materials Science and Metallurgy, University of Cambridge
Pembroke Street, CB2 3 QZ, England, United Kingdom
[3]Department of Physics, Faculty of Science, Universiti Putra Malaysia
43400 UPM Serdang, Malaysia

[a]noorhana_yahya@petronas.com.my

Keywords: Single crystals, saturation magnetization, sol-gel

Abstract. Magnetic properties of nano-crystalline yttrium iron garnet, $Y_3Fe_5O_{12}$ and bismuth iron garnet, $Bi_3Fe_5O_{12}$ were studied. The samples were synthesized by using sol gel route. The gel were prepared using nitrates of yttrium and iron for the yttium iron garnet (YIG) and nitrates of bismuth and iron for the bismuth iron garnet (BIG). The raw materials were mixed and dissolved in citric acid and were stirred for 3 months in room temperature until the gel was observed. The X-ray diffraction pattern reveals the cubic structure of YIG and BIG samples at 700^0C and 500^0C respectively. From the M-H diagrams it was found that the YIG and BIG samples have saturation magnetization, Ms of 27.2 Gs with rectangular hysteresis loop and 24.4 Gs with S hysteresis loop, respectively. It is evident from the FESEM micrographs that the rectangular loop shape (YIG) arises from the homogeneous and rounded microstructure as compared to the inhomogenous and random orientation microstructure (BIG) of the samples. From the Electron diffraction done on Transmission Electron Microscope, both of the samples were shown to be single crystals.

Introduction

Magnetic garnet, namely, yttrium iron garnet ($Y_3Fe_5O_{12}$) and bismuth iron garnet ($Bi_3Fe_5O_{12}$) that belongs to a group of magnetic oxides, is an attractive material for magneto-optical devices. They also have important applications within microwave frequencies, namely, optical isolators, oscillators, circulators and others, due to their large Faraday rotation and high saturation magnetization [1, 2]. For these reasons, there are ongoing interests in investigating the chemical, physical and magnetic properties of these garnet materials. Extensive studies have been carried out on the synthesis of YIG nano-particles by coprecipitation technique. Due to the novel processing method, these oxides possess unique magnetic, magneto optical, thermal, electrical and mechanical properties such as excellent creep and radiation damage resistance, high thermal conductivity, high electrical resistivity, controllable saturation magnetization, moderate thermal expansion coefficient, energy transfer efficiency and narrow line width in ferromagnetic resonance [3]. Recently, YIG nanocrystals that were dispersed on glass have been investigated for high density magnetic or magneto-optical information storage [4].

The properties of materials composed of magnetic nanoparticles are results of both the intrinsic and the extrinsic properties of the particles [5]. Studies on magnetic properties as a function of particle size have gained much interest particularly those within nanometer range. Below some critical dimension, magnetic particles become single domain and show superparamagnetic (SPM) behaviour [6,7]. It is now widely accepted that three-dimensional (3D) random distribution of nearly monodisperse single domain magnetic nanoparticles (superspins) with appreciable interparticle interactions exhibits a magnetic phase transition from pure N'eel–Brown-type

superparamagnetic to a collective superspin glass (SSG) state at low temperature [8]. On the other hand, ferromagnetic (FM) ordering has been reported to exist in one- (1D) and two-dimensional (2D) self-organized or regular arrays of FM nanoparticles [9]. Some magnetic performances such as coercive force and initial permeability are strongly dependent on the microstructural aspects, i.e. the synthesis method and the conditions of further annealing and grinding [10].

Recently, chemical methods have been used successfully to prepare homogeneous and fine reproducible ferrite powders [11]. Samples with particle size ranging from 45nm to 450nm were obtained using a sol gel technique [12]. This technique involves a set of chemical reactions which irreversibly convert a homogeneous solution of molecular reactant precursors (a sol) into an infinite molecular weight three-dimensional polymer (a gel) forming an elastic solid filling the same volume of solution [13,14]. Typically this involves a hydrolysis reaction followed by polymerization. This work premise deals with the preparation of yttrium iron garnet and bismuth iron garnet via aqueous sol gel technique. A tedious preparation route was taken where room temperature sol to gel reaction was done for three months. This earnest effort was taken to ensure the formation of gel self assembly. The magnetic properties and the microstructure of the nanoparticles were studied. We hope that the result of this work can be used to develop magnetic sensors with improved sensitivity, smaller size and compatible with electronic systems.

Experimental

The raw materials used for this sol-gel method are high purity (99.99%) yttrium nitrate, $Y(NO_3)_3.6H_2O$, bismuth nitrate, $Bi(NO_3)_3.5H_2O$ and ferum nitrate, $Fe(NO_3)_3.9H_2O$.

The chemical reaction can be expressed as follows:

For yttrium iron garnet

$$3Y(NO_3)_3.6H_2O + 5Fe(NO_3)_3.9H_2O \longrightarrow Y_3Fe_5O_{12} + \text{complexes}$$

For bismuth iron garnet

$$3Bi(NO_3)_3.5H_2O + 5Fe(NO_3)_3.9H_2O \longrightarrow Bi_3Fe_5O_{12} + \text{complexes}$$

Appropriate amount of yttrium nitrate and bismuth nitrate and were dissolved in an aqueous solution of citric acid. The nitrates were dissolved by stirring at 300 r.p.m at room temperature for 3 months to ensure homogeneous solution. The stirring was continued until the viscosity of solution increased and resulting to formation of gel. When the gel was formed, the hot plate was heated up to 60^{o}C and left for another 6 hours to change the viscous solution to a clear and wet gel. The samples were heated at 105 ^{o}C for 24 hours to remove the water content.

After the drying process, both samples were pre-sintered using carbolite furnace at 300^{o}C for 2 hours in air. All the pre-sintered powders were then wet crushed for 6 hours using Planetary Micromill to obtain fine particles. After 6 hours of wet crushing, the resulting mass was dried in an oven at 105^{o}C for 24 hours to evaporate the water. Both samples were then crushed into fine powder. This is important to facilitate the solid state reaction in the final sintering process [13,14].

The powder was formed into pellet and toroid. 1.5 wt% of polivinyle alcohol (PVA) acting as binder and 1.5wt % of zinc stearate acting as lubricant were added into the green garnet powders. A hydraulic press with 60 kN force was used to form a pellet and a toroidal shaped samples. This process is important to obtain a uniform compact. Subsequently, they were sintered at 600^{0}C, 700ºC, 800ºC, and 900ºC for 3 hours in air. This procedure was done to study the amorphous to crystal state profile. The green powders were characterized by x-ray diffraction (Philips, X'pert PRO PW 3040 PAN Analytical) to confirm the best garnet phase. A field emission scanning electron microscopy (FESEM, SUPRA 35VP), a low resolution transmission electron microscope (JOEL JEM CX 200) and a high resolution transmission electron microscope (FEI Tecnai F20) with

200kV field emission gun (FEG), were used to study the morphology and the d-spacing of some of the samples. Hysteresis loop studies were conducted by using vibrating sample magnetometer DMS-VSM. The sample is fixed to a small sample holder located at the end of a sample rod mounted in an electromechanical transducer which was driven by a power amplifier at 90 Hertz. The average crystallite sizes of the synthesized powders were determined using the X-ray broadening of the (4 2 0) diffraction peak by the well-known Scherrer equation:

$$D = \frac{0.9\lambda}{\beta \cos\theta}$$

where D is crystallite size in nm, λ the radiation wave length (0.15405 nm for Cu Kα), β the corrected full width at half maximum and θ is the diffraction angle.

Results and Discussions

Figure 1 shows the XRD pattern obtained for the YIG samples. It is clearly seen that samples that the samples heated at 300°C, 400°C, 500°C and 600°C are mainly amorphous. It was found that amorphous-gel-to-crystalline phase transition of yttrium iron garnet was formed at 700^{0}C. This is observed by the sharp and high density diffraction patterns. The lower crystallization temperature as compared to those of the conventional technique could be related to the good homogeneity of the as-prepared gel. It should be noted that the highest peak appeared at 32.2521° with 3718 counts of the 2θ. From the graph, it is observed that the diffracted prominent peaks at the (420), (400) and (422) plane are observed at the corresponding angle as reported in the standard. The observed values of the diffraction patterns were in good agreement with standard values in JCPDS card file number: 00 – 0033- 0693 confirming the formation of cubic garnet. These peaks were also previously observed by other researchers [7,12,15]. It is obvious that the correct sintering temperature is one of the main factors affecting the formation of the garnet phase for all the samples. From the XRD profile and using the Scherrer equation it was found that the particle size of the YIG samples is 58 nm (Table 1).

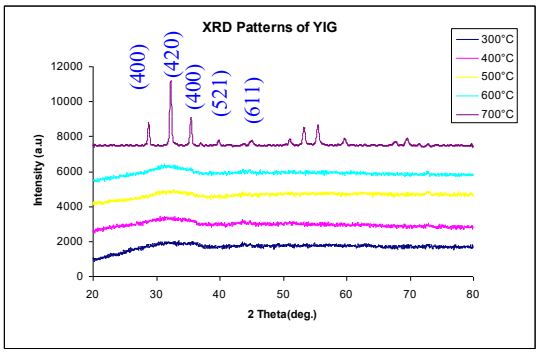

Fig. 1: X-Ray Diffraction Profile for the YIG samples sintered at 300^{0}C, 400^{0}C, 500^{0}C, 600^{0}C and 700^{0}C for 2 hours in air.

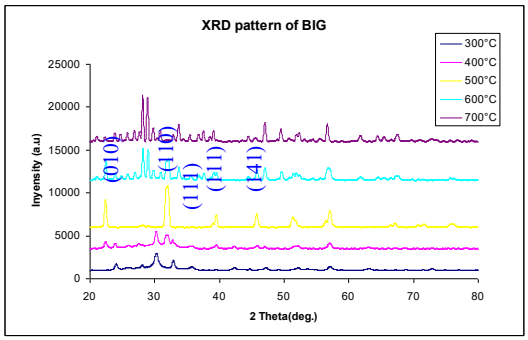

Fig. 2: X-Ray Diffraction Profile for the BIG samples sintered at 300^{0}C, 400^{0}C, 500^{0}C, 600^{0}C and 700^{0}C for 2 hours in air.

Figure 2 shows the XRD pattern obtained for sample BIG with different sintering temperature. The sintered powder that was heated at 300°C and 400°C exhibit some small diffraction peaks. More interesting is at 500°C, clear diffraction peaks indicating the crystalline transition phase. This low sintering temperature for the formation of the single phase garnet is higher than that by the conventional method. Above the crystallization temperatures of the BIG sample, 600^{0}C and 700^{0}C, unknown peaks appeared that cannot be attributed to any phases formed in our composition. The major peak with the plane (110) of the 2θ for sample at 500°C was shifted significantly. The highest peak achieved for the single phase BIG sample appeared at 32.0786° with 4766 counts of the 2θ. From the graph, it can be observed that the Miller Indices matched well with

the diffractions reported by the standard in the JCPDS card file number: 01-073-0548 confirming the formation of the cubic garnet. The d-spacing of the YIG and BIG samples are 2.78 Å and 2.79Å respectively (Table 1).

Figure 3 shows the M-H behaviour of the YIG sample measured at room temperature. The YIG sample shows saturation magnetization of 27.20 Gs and a coercivity of 23.65 Oe. Magnetic saturation was obtained at very low field indicating the soft magnetic nature of sample. The pure YIG materials need very high sintering temperature, in this case 700^0C, to achieve high enough density and good magnetic properties. The EDX spectrum (Figure 4) shows the presence of elements such yttrium, iron and oxygen with the atomic percent 16.18, 27.99 and 55.83 respectively. The amount of each element matches with the sample composition in which the amount of oxygen is the highest followed by iron and yttrium. A significant peak attributed to gold at 2.15 eV (used for the sample coating) was also observed. The chemical composition of the powders was estimated via a semi-quantitative analysis of the intensity of the EDX spectrum.

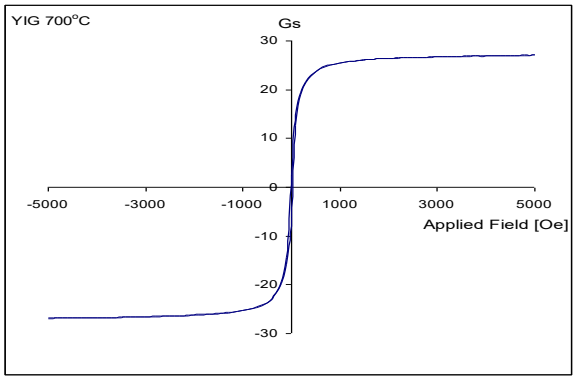

Fig. 3: M-H behaviour of the YIG sample sintered at 700°C for 2 hours.

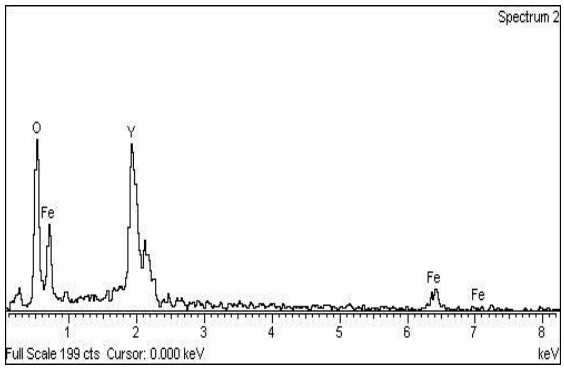

Fig. 4: EDX profile of the YIG sample sintered at 700°C for 2 hours.

Referring to Fig. 5, the saturation magnetization of sample BIG is 24.41 Gs and the coercivity obtained is 21.25 Oe. These values are lower than that compared to sample YIG. The magnetic moment of the nanoparticles strongly depends on the particle size. There is a slight reduction in the particle size (14 %) and saturation magnetization (14%) comparing YIG to BIG samples (Table 1). The decrease in particle size increases the surface to volume ratio, and more magnetic ions located at the particle surface cause the surface uncompensated magnetic moments to become significant for the net magnetization [16]. The EDX spectrum in Figure 6 shows the presence of bismuth, iron and oxygen elements with the atomic percent 19.24, 28.45 and 52.31 respectively. The amount of each element matches with the sample composition in which the amount of oxygen is the highest followed by iron and bismuth. The gold element can also be observed.

Table 1: Analysis of X-ray diffraction and Magnetization for YIG and BIG samples measured at room temperature

Sample	XRD				Magnetization	
	2 Theta (°)	d-spacing (Å)	Counts	Grain size (nm)	Ms (Gs)	Hc (Oe)
YIG	32.25	2.78	3718	58	27.20	23.65
BIG	32.08	2.79	4766	50	24.41	21.25

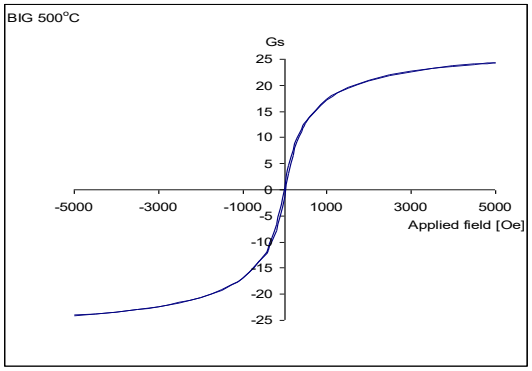

Fig. 5: M-H behavior of the BIG sample with sintering temperature of 700°C for 2 hours.

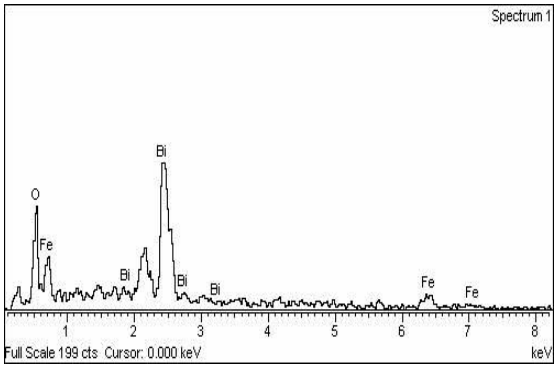

Fig. 6: EDX profile of the BIG sample with sintering temperature of 700°C for 2 hours.

Having a closer look at the hysteresis loop (Fig. 3 and Fig. 5) it is obvious that the YIG sample exhibits a rectangular hysteresis while the BIG sample showed normal hysteresis loop. Hysteresis losses are due to energy losses from non-reversible wall motion proportional to the area of the M-H hysteresis cycle [17]. It is obvious that the area of the loop for both samples is small or rather negligible. This is due to the nanoparticle size of the samples. The rectangular loop for sample YIG indicates the consistency of the microstructure and grain size. Observing the SEM image of the YIG sample from Fig. 7 it is observed that homogeneous microstructure was achieved with regular spherical size of the grains promoting the ability of the magnetic spins to hold the magnetic alignment at higher external field. The electron diffraction pattern attached to FESEM image indicates the single crystal structure achieved due sol gel soft chemistry route taken in this work. It was also reported that besides the extrinsic factor, a square loop hysteresis can be expected when high magnetocrystalline and zero magnetostriction are present. The important characteristics of the rectangular looped garnet are high M/H squareness ratio, controlled coercive force (H_c) and low switching time [17] enabling the materials to behave as a good magnetic sensor. The normal S - shaped hysteresis indicates randomly oriented crystals where the magnetostriction energy is greater that the magnetocrystalline energy. From Figure 8 it could be observed that the BIG sample showed various shape distribution such as sheet, agglomerate and some traces of rod shaped microstructure. The microstructure shown is consistent with the hysteresis results obtained from Fig. 3 and Fig. 5.

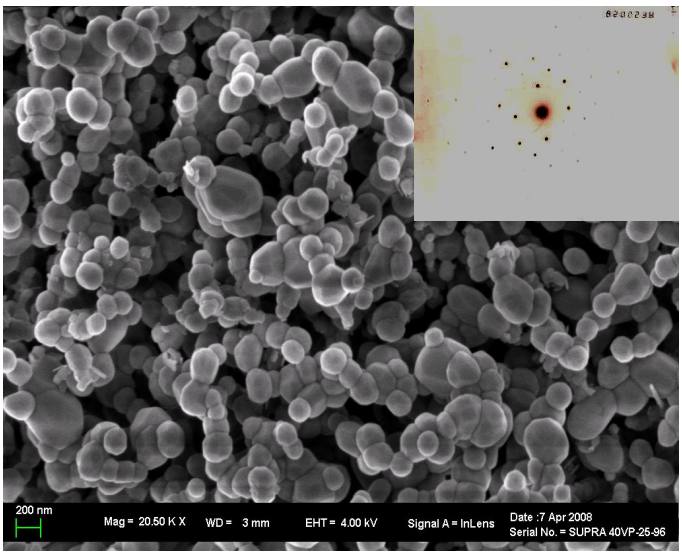

Fig. 7: Field Emission Scanning Electron Microscopy (FESEM) and Electron Diffraction (ED) images of sample YIG.

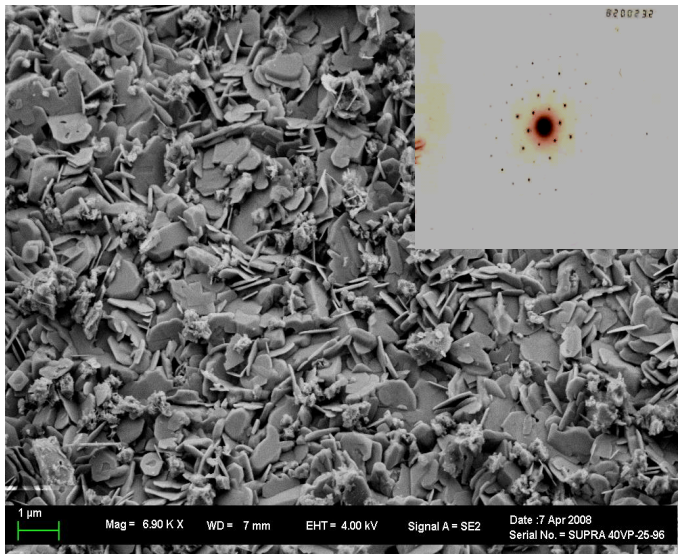

Fig. 8: Field Emission Scanning Electron Microscopy (FESEM) and Electron Diffraction (ED) images of sample BIG.

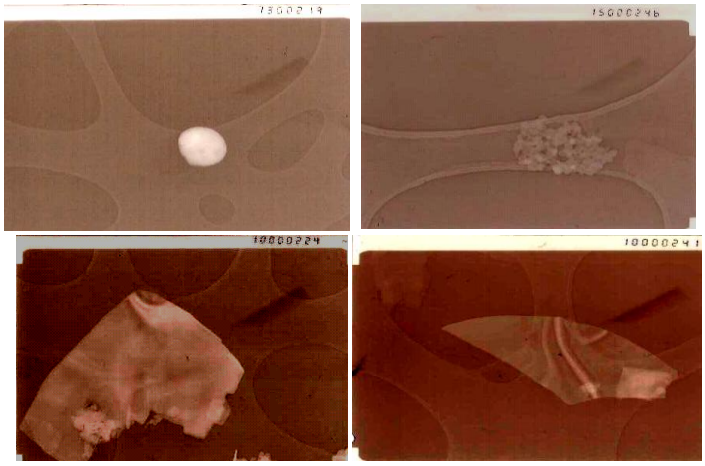

Fig. 9: Transmission Electron Microscopy (TEM) images (a) YIG particulate (b) YIG agglomerate (c) BIG sheet (d) BIG sheet.

Transmission electron microscope (TEM) was done to rectify the shapes of the YIG and BIG powders. It was found that the FESEM images and the TEM images are consistent whereby the YIG samples are mostly spherical shaped morphology (Figure 9 (a) and (b) whilst the BIG powders are mostly nanosheet (Figure 9 (c) and (d)). The speculation made on the hysteresis shape for both the samples as such is convincing.

Conclusion

XRD and TEM results show that the samples have single phase and single crystal garnet structure while the crystallization occurs at 700^{o}C and 500^{o}C for YIG and BIG samples respectively. This lower crystallization temperature and short sintering time (2 hours) could be related to the good homogeneity of the gel preparation via the soft chemistry route taken in this work. The magnetizations M-H for both samples were measured at room temperature. The YIG sample shows saturation magnetisation of 27.20 Gs and coercive force of 23.65 Oe while BIG sample exhibit 24.41 Gs for the saturation magnetization and 21.25 Oe for the coercive force. The magnetic

moment of nanoparticles strongly depends on the particle size. The rectangular shaped hysteresis loop for the YIG sample is due to the homogeneous morphology microstructure and promises to be a good magnetic sensor with fast switching time.

Acknowledgement
The authors thank the Ministry of Science, Technology and Innovation for the fund provided under IRPA grant 54430 and Academy Science of Malaysia for the SAGA grant. The authors thank the University of Cambridge for the work done on the Transmission Electron Microscope.

References

[1] M. Ristić, I. Nowik, S. Popović, I. Felner, S. Musić: Mater. Lett. Vol. 57 (2003), p. 2584.

[2] C.S. Kuroda, T.Y. Kim, T. Hirano, K. Yosh, T. Namikawa and Y. Yamazaki: Electrochem. Acta Vol. 44 (1999), p. 3921.

[3] E. Garskaite, K. Gibson, A. Leleckaite, J. Glaser, D. Niznansky, A. Kareiva, H.-J. Meyer: Chem. Phys. Vol. 323 (2006), p. 204.

[4] S. Taketomi, C.M. Sorensen, K.J. Klabunde: J. Magn. Magn. Mater. Vol. 222 (2000), p. 54.

[5] R.H. Kodama: J. Magn. Magn. Mater. Vol. 200 (1999), p. 359.

[6] A.E. Berkowitz, R.H. Kodama, A. Makhlouf, Salah, F.T. Parker, F.E. Spada, E.J. McNiff Jr. and S. Foner: J. Magn. Magn. Mater. Vols. 196-197 (1999), p. 591.

[7] E. Tronc et al.: J. Magn. Magn. Mater. (2003), p. 262.

[8] S. Sahoo, O. Petracic, W. Kleemann, P. Nordblad, S. Cardoso and P.P. Freitas: J. Magn. Magn. Mater. Vols. 272–276 (2004), p. 1316.

[9] S. Sahoo, O. Sichelschmidt, O. Petracic, Ch. Binek, W. Kleemann, G.N. Kakazei, Yu.G. Pogorelov, J.B. Sousa, S. Cardoso, P.P. Freitas: J. Magn. Magn. Mater. Vol. 240 (2002), p. 433.

[10] P. Vaqueiro, M.A. Lopez-Quintela, J. Rivas, J.M. Greneche: J. Magn. Magn. Mater. Vol. 169 (1997), p. 56.

[11] R.V. Mangalajara, S. Ananthakuma, P. Manohar and F.D. Gnaman: Powder Characteristics, Sintering Behaviour and Microstructure of NiZn Derived through Citrate-Gel Decomposition Technique, (2000) Digests of ICF 8: 207

[12] R.D. Sancheza, J. Rivasb, P. Vaqueiroc, M.A. Lopez-Quintelad, D. Caeirob: J. Magn. Magn. Mater. (2001), p. 278.

[13] P. Vaqueiro, M.P. Crosnier – Lopez and M.A. Lopez – Quintela: J. Solid State Chem. Vol. 126 (1996), p. 161.

[14] J.-L. Rehspringer, J. Bursik, D. Niznansky, A. Klarikova: J. Magn. Magn. Mater. Vol. 211 (2000), p. 291.

[16] M. Rajendran, S. Deka, P.A. Joy and A.K. Bhattacharya: J. Magn. Magn. Mater. Vol. 301 (2006), p. 212.

[15] N. Yahya and K.H Goh: Am. J. Appl. Sci. Vol. 4 (2007), p. 80.

[16] E.P Wolfarth, Ferromagnetic Materials, North Holland Publishing Co., (1980) p. 224-233.